Reactions of $(Me_3ECH_2)_3ZrSi(SiMe_3)_3$ (E = C, Si) with 2,6-Dimethylphenyl Isocyanide. Preferential Isocyanide Insertion into Zr−Silyl Bonds

Zhongzhi Wu, Lenore H. McAlexander, Jonathan B. Diminnie, and Ziling Xue*

Department of Chemistry, The University of Tennessee, Knoxville, Tennessee 37996-1600

Received June 11, 1998

The reactions of alkyl silyl complexes $(Me_3ECH_2)_3ZrSi(SiMe_3)_3$ [E = C (**1**), Si (**2**)] with 2,6-dimethylphenyl isocyanide (ArNC) have been investigated. The first ArNC was found to insert exclusively into the *Zr−Si* bond, and the second and third ArNC into the Zr−C bonds in **1** and **2**. **1** and **2** react with up to 3 equiv of ArNC to give $(Me_3ECH_2)_3Zr\{\eta^2\text{-}C[Si(SiMe_3)_3]{=}NAr\}$ [E = C (**3**), Si (**4**)], $(Me_3ECH_2)_2Zr[\eta^2\text{-}C(CH_2EMe_3){=}NAr]\{\eta^2\text{-}C[Si(SiMe_3)_3]{=}NAr\}$ [E = C (**5**), Si (**6**)], and $(Me_3ECH_2)Zr[\eta^2\text{-}C(CH_2EMe_3){=}NAr]_2\{\eta^2\text{-}C[Si(SiMe_3)_3]{=}NAr\}$ [E = C (**7**), Si (**8**)]. The tri-insertion complexes **7** and **8** are inert to excess ArNC. The structures of **3** and **7** have been determined by X-ray crystallography. In the structure of **3**, the α-hydrogen atoms on one neopentyl ligand lie in close contact (av 2.41 Å) with the metal center giving rise to Zr−C−Hα bond angles of 90 and 92°. The crystal structure of the precursor **1** has also been determined.

Introduction

Early-transition-metal silyl chemistry is becoming increasingly prominent in organometallic chemistry.[1,2] Group 4 d^0 metal silyl complexes can undergo insertion reactions[2c,k,3,4] and catalyze silane polymerizations[1g,2a,b,5] and hydrosilation of alkenes and alkynes.[6] However, most reactivity studies of d^0 early-transition-metal silyl complexes have been conducted on those containing π-anionic ligands such as η^5-cyclopentadienyl (Cp).[1,2] Our research has been focused on the chemistry of Cp-free d^0 early-transition-metal complexes, such as alkyl silyl complexes.[7] These electronically and coordinatively unsaturated complexes present a new and unique opportunity to directly compare the relative reactivities of alkyl and silyl ligands.

Insertions of isocyanides (RNC) and CO into M−C bonds are well documented.[8] The accepted mechanism involves addition of CO or RNC to the metal center, followed by migration of a ligand onto the carbonyl or isocyanide carbon atoms (Scheme 1). Such insertions into M−silyl bonds in the absence of alkyl ligands have been reported by Tilley, Mori, and co-workers.[3,9] For example, $Cp_2Zr[Si(SiMe_3)_3]Cl$,[3b] $CpCp^*Zr[Si(SiMe_3)_3]Cl$,[3e] $(Me_3CO)_3ZrSi(SiMe_3)_3$,[3f] $(2,6\text{-}{}^iPr_2C_6H_3N)_2Mo[Si(SiMe_3)_3]Cl$,[9a] and $Cp_2ScSi(SiMe_3)_3$[9c] undergo 2,6-dimethylphenyl

* To whom correspondence should be addressed. Fax: (423) 974-3454. E-mail: xue@utk.edu.

(1) (a) Tilley, T. D. In *The Chemistry of Organic Silicon Compounds*; Patai, S., Rappoport, Z., Eds.; Wiley: New York, 1989; Chapter 24. (b) Tilley, T. D. In *The Silicon−Heteroatom Bond*; Patai, S., Rappoport, Z., Eds.; Wiley: New York, 1991; Chapters 9 and 10. (c) Tilley, T. D. *Comments Inorg. Chem.* **1990**, *10*, 37. (d) Harrod, J. F.; Mu, Y.; Samuel, E. *Polyhedron* **1991**, *11*, 1239. (e) Corey, J. Y. In *Advances in Silicon Chemistry*; Larson, G., Ed.; JAI Press: Greenwich, CT, 1991; Vol. 1, p 327. (f) Xue, Z. *Comments Inorg. Chem.* **1996**, *18*, 223. (g) Tilley, T. D. *Acc. Chem. Res.* **1993**, *26*, 22. (h) Sharma, H. K.; Pannell, K. H. *Chem. Rev.* **1995**, *95*, 1351.

(2) (a) Woo, H.-G.; Walzer, J. F.; Tilley, T. D. *J. Am. Chem. Soc.* **1992**, *114*, 7047. (b) Imori, T.; Tilley, T. D. *Polyhedron* **1994**, *13*, 2231. (c) Radu, N. S.; Engeler, M. P.; Gerlach, C. P.; Tilley, T. D.; Rheingold, A. L. *J. Am. Chem. Soc.* **1995**, *117*, 3621. (d) Xin, S. X.; Harrod, J. F. *J. Organomet. Chem.* **1995**, *499*, 181. (e) Dioumaev, V. K.; Harrod, J. F. *J. Organomet. Chem.* **1996**, *521*, 133. (f) Dioumaev, V. K.; Harrod, J. F. *Organometallics* **1996**, *15*, 3859. (g) Hao, L. J.; Lebuis, A. M.; Harrod, J. F.; Samuel, E. *J. Chem. Soc., Chem. Commun.* **1997**, 2193. (h) Dioumaev, V. K.; Harrod, J. F. *Organometallics* **1997**, *16*, 2798. (i) Jiang, Q.; Pestana, D. C.; Carroll, P. J.; Berry, D. H. *Organometallics* **1994**, *13*, 3679. (j) Procopio, L. J.; Carroll, P. J.; Berry, D. H. *Polyhedron* **1995**, *14*, 45. (k) Corey, J. Y.; Rooney, S. M. *J. Organomet. Chem.* **1996**, *521*, 75. (l) Shaltout, R. M.; Corey, J. Y. *Organometallics* **1996**, *15*, 2866. (m) Huhmann, J. L.; Corey, J. Y.; Rath, N. P. *J. Organomet. Chem.* **1997**, *533*, 61. (n) Hengge, E.; Gspaltl, P.; Pinter, E. *J. Organomet. Chem.* **1996**, *521*, 145. (o) Banovetz, J. P.; Suzuki, H.; Waymouth, R. M. *Organometallics* **1993**, *12*, 4700. (p) Spaltenstein, E.; Palma, P.; Kreutzer, K. A.; Willoughby, C. A.; Davis, W. M.; Buchwald, S. L. *J. Am. Chem. Soc.* **1994**, *116*, 10308. (q) Verdaguer, X.; Lange, U. E. W.; Reding, M. T.; Buchwald, S. L. *J. Am. Chem. Soc.* **1996**, *118*, 6784. (r) Fu, P. F.; Marks, T. J. *J. Am. Chem. Soc.* **1995**, *117*, 10747. (s) Schumann, H.; Meese-Marktscheffel, J. A.; Hahn, F. E. *J. Organomet. Chem.* **1990**, *390*, 301. (t) Molander, G. A.; Nichols, P. J. *J. Am. Chem. Soc.* **1995**, *117*, 4415. (u) Takahashi, T.; Hasegawa, M.; Suzuki, N.; Saburi, M.; Rousset, C. J.; Fanwick, P. E.; Negishi, E. *J. Am. Chem. Soc.* **1991**, *113*, 8564.

(3) (a) Tilley, T. D. *J. Am. Chem. Soc.* **1985**, *107*, 4084. (b) Campion, B. K.; Falk, J.; Tilley, T. D. *J. Am. Chem. Soc.* **1987**, *109*, 2049. (c) Elsner, F. H.; Woo, H.-G.; Tilley, T. D. *J. Am. Chem. Soc.* **1988**, *110*, 313. (d) Arnold, J.; Engeler, M. P.; Elsner, F. H.; Heyn, R. H.; Tilley, T. D. *Organometallics* **1989**, *8*, 2284. (e) Elsner, F. H.; Tilley, T. D.; Rheingold, A. L.; Geib, S. *J. Organomet. Chem.* **1988**, *358*, 169. (f) Heyn, R. H.; Tilley, T. D. *Inorg. Chem.* **1989**, *28*, 1768.

(4) Procopio, L. J.; Carroll, P. J.; Berry, D. H. *Organometallics* **1993**, *12*, 3087.

(5) (a) Aitken, C. T.; Harrod, J. F.; Samuel, E. *J. Am. Chem. Soc.* **1986,** *108*, 4059. (b) Aitken, C. T.; Barry, J.-P.; Gauvin, F.; Harrod, J. F.; Malek, A.; Rousseau, D. *Organometallics* **1989**, *8*, 1732. (c) Mu, Y.; Aitken, C. T.; Cote, B.; Harrod, J. F.; Samuel, E. *Can. J. Chem.* **1991**, *69*, 264. (d) Harrod, J. F. In *Inorganic and Organometallic Polymers with Special Properties*; NATO ASI Series E; Laine, R. M., Ed.; Kluwer Academic Publishers: Amsterdam, 1991; Vol. 206, p 87.

(6) (a) Corey, J. Y.; Zhu, X. H. *Organometallics* **1992**, *11*, 672. (b) Kesti, M. R.; Waymouth, R. M. *Organometallics* **1992**, *11*, 1095.

(7) (a) Xue, Z.; Li, L.; Hoyt, L. K.; Diminnie, J. B.; Pollitte, J. L. *J. Am. Chem. Soc.* **1994**, *116*, 2169. (b) McAlexander, L. H.; Hung, M.; Li, L.; Diminnie, J. B.; Xue, Z.; Yap, G. P. A.; Rheingold, A. L. *Organometallics* **1996**, *15*, 5231. (c) Diminnie, J. B.; Hall, H. D.; Xue, Z. *J. Chem. Soc., Chem. Commun.* **1996**, 2383. (d) Li, L.; Diminnie, J. B.; Liu, X.; Pollitte, J. L.; Xue, Z. *Organometallics* **1996**, *15*, 3520. (e) Diminnie, J. B.; Xue, Z. *J. Am. Chem. Soc.* **1997,** *119*, 12657.

(8) Durfee, L. D.; Rothwell, J. P. *Chem. Rev.* **1988**, *88*, 1059.

10.1021/om980485o CCC: $15.00
Publication on Web 10/08/1998

Scheme 1

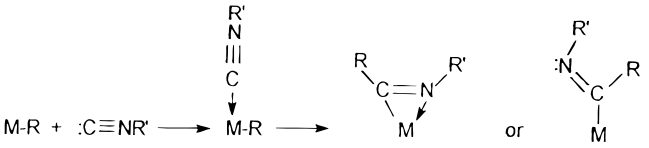

isocyanide (ArNC) insertion into M−Si bonds to form iminosilaacyl complexes. Insertion and addition of more than 1 equiv of isocyanide to early-transition-metal alkyl complexes have also been observed. Wilkinson and co-workers[10] reported that in the reaction of $(Me_3CCH_2)_4$-Zr with Bu^{t}NC, the complex undergoes isocyanide insertion into one of the M−C bonds, followed by addition of a second Bu^{t}NC without subsequent migration of an alkyl ligand. The failure of the remaining alkyl groups to migrate to the isocyanide carbon atom was attributed to steric congestion. Multiple isocyanide insertions to M−alkyl bonds were observed by Rothwell and co-workers[8,11] in the reaction of $(R'O)_{4-x}MR_x$ (x = 2, 3; M = Ti, Zr, Hf) with 2 or 3 equiv of isocyanide; all M−C bonds undergo isocyanide insertion. Heating of the products leads to the coupling of the isocyanide ligands to form metallacyclic compounds.[12] Similar reactions were also recently observed between 2 equiv of isocyanide and $[(C_5Me_4)SiMe_2(NBu^t)]ZrMe_2$,[13] [M(TC-3,$n$)-$R_2$] [TC = tropocoronand; M = Zr(IV), Hf(IV); n = 3, 5; R = CH_2Ph, Ph][14] and [p-Bu^t-calix[4]-$(OMe)_2(O)_2ZrR_2$] (R = Me, CH_2Ph, p-MeC_6H_4).[15] However, to our knowledge, there are only two reports of the reactions of isocyanides with metal complexes containing different reactive ligands.[16] Our metal alkyl silyl complexes $(Me_3ECH_2)_3ZrSi(SiMe_3)_3$ [E = C (**1**), Si (**2**)] offer a unique opportunity to observe the direct competition between silyl and alkyl ligands in the migration step, and to study whether silyl or alkyl ligand migration is preferred. In this paper, we report our investigations of the reactions between 2,6-dimethylphenyl isocyanide and $(Me_3ECH_2)_3ZrSi(SiMe_3)_3$.

Experimental Section

General Procedures. All manipulations were performed under a dry nitrogen atmosphere with the use of either standard Schlenk techniques or a glovebox. Solvents were purified by distillation over potassium/benzophenone ketyl. Benzene-d_6 was dried over activated molecular sieves and stored under nitrogen. 2,6-Dimethylphenyl isocyanide (Fluka) was used as received. $(Me_3ECH_2)_3ZrSi(SiMe_3)_3$ [E = C (**1**), Si (**2**)] were prepared by the reactions of $(Me_3ECH_2)_3ZrCl$ with $Li(THF)_3Si(SiMe_3)_3$.[7b] Infrared spectra were recorded on a Bio-Rad FST-60A infrared spectrometer. NMR spectra were recorded on a Bruker AC-250 or AMX-400 Fourier transform spectrometer and referenced to solvents (residual protons in the ^{1}H spectra). Elemental analyses were performed by E+R Microanalytical Laboratory (Corona, NY).

$(Me_3CCH_2)_3Zr\{\eta^2$-C[Si(SiMe$_3$)$_3$]=NAr$\}$ (3). A solution of 0.21 g (0.38 mmol) of **1** in toluene (2 mL) at room temperature was treated dropwise with a solution of 0.049 g (0.38 mmol) of ArNC in toluene (2 mL) over a period of 10 min. The solution was then stirred at room temperature for 1 h. The bright yellow solution was then concentrated and cooled to −18 °C, producing 0.15 g of **3** as bright yellow crystals (58% yield) suitable for X-ray analysis. IR (KBr, cm^{-1}): 2950 s, 2861 s, 2790 m, 2700 w, 1579 w, 1509 s, 1462 s, 1443 m sh, 1356 s, 1229 s, 1169 w, 1090 w, 996 w, 832 s, 773 s, 689 s, 623 s, 524 w. ^{1}H NMR (benzene-d_6, 250 MHz, 23 °C): δ 6.95, 6.89 (3H, C_6H_3), 1.96 (s, 6H, $C_6H_3Me_2$), 1.23 (s, 27H, CH_2CMe_3), 1.21 (s, 6H, CH_2CMe_3), 0.22 [s, 27H, Si(SiMe_3)$_3$]. ^{13}C{^{1}H} NMR (benzene-d_6, 62.9 MHz, 23 °C): δ 296.0 (C=N), 155.9, 129.0, 127.6, 126.4 (C_6H_3), 95.0 (CH_2CMe_3), 35.5 (CH_2CMe_3), 35.0 (CH_2CMe_3), 19.6 ($C_6H_3Me_2$), 2.6 [Si(SiMe_3)$_3$] Anal. Calcd for $C_{33}H_{69}NSi_4Zr$: C, 57.99; H, 10.18. Found: C, 57.63; H, 10.04.

$(Me_3SiCH_2)_3Zr\{\eta^2$-C[Si(SiMe$_3$)$_3$]=NAr$\}$ (4). To a pale-yellow solution of **2** (0.12 g, 0.20 mmol) in toluene (2 mL) was added slowly 1 equiv of ArNC (0.026 g, 0.20 mmol) in toluene (2 mL) at room temperature over 10 min. The bright-yellow solution was concentrated and cooled to −18 °C to afford 0.10 g of **4** as yellow crystals (69% yield). ^{1}H NMR (benzene-d_6, 250 MHz, 23 °C): δ 6.95, 6.89 (3H, C_6H_3), 1.96 (s, 6H, $C_6H_3Me_2$), 0.78 (s, 6H, CH_2SiMe_3), 0.24 [s, 27H, Si(SiMe_3)$_3$], 0.18 (s, 27H, CH_2SiMe_3). ^{13}C{^{1}H} NMR (benzene-d_6, 62.9 MHz, 23 °C): δ 297.5 (C=N), 155.3, 129.1, 127.4, 126.6 (C_6H_3), 65.7 (CH_2-$SiMe_3$), 19.4 ($C_6H_3Me_2$), 3.1 (CH_2SiMe_3), 2.4 [Si(SiMe_3)$_3$]. Anal. Calcd for $C_{30}H_{69}NSi_7Zr$: C, 49.25; H, 9.50. Found: C, 49.52; H, 9.68.

$(Me_3CCH_2)Zr[\eta^2$-C(CH_2CMe_3)=NAr$]_2\{\eta^2$-C[Si(SiMe$_3$)$_3$]=NAr$\}$ (7). To a solution of 50 mg (0.09 mmol) of **1** in benzene-d_6 was added 36 mg (0.27 mmol) of ArNC. The clear, bright-yellow solution in an NMR tube was then allowed to evaporate slowly at room temperature. After several days, 50 mg of **7** were isolated as yellow crystals (58% yield), which were used for X-ray crystal structure determination and elemental analysis. ^{1}H NMR (benzene-d_6, 250 MHz, 23 °C): δ 6.94, 6.89 (m, 9H, C_6H_3), 2.44 (d, $^2J_{H-H}$ = 15.2 Hz, 2H, $NCCH_aH_bCMe_3$), 2.32 (d, 2H, $NCCH_aH_bCMe_3$), 2.06 (s, 6H, $C_6H_3Me_2$), 2.03 (s, 6H, $C_6H_3Me_2$), 1.96 (s, 6H, $C_6H_3Me_2$), 1.44 (s, 2H, $ZrCH_2CMe_3$), 1.14 (s, 9H, $ZrCH_2CMe_3$), 0.94 (s, 18H, N=CCH_2CMe_3), 0.31 [s, 27H, Si(SiMe_3)$_3$]. ^{13}C{^{1}H} NMR (benzene-d_6, 62.9 MHz, 23 °C): δ 298.8 [N=CSi(SiMe$_3$)$_3$], 261.0 (N=CCH_2CMe_3), 155.4, 150.2, 129.3, 128.9, 128.4, 127.8, 125.6, 125.3 (C_6H_3), 75.3 ($ZrCH_2CMe_3$), 53.3 (N=CCH_2CMe_3), 36.4 ($ZrCH_2CMe_3$), 35.6 ($ZrCH_2CMe_3$), 31.6 (N=CCH_2CMe_3), 31.1 (N=CCH_2CMe_3), 20.9 ($C_6H_3Me_2$), 20.4 ($C_6H_3Me_2$), 20.3 ($C_6H_3Me_2$), 3.5 [Si(SiMe_3)$_3$]. Anal. Calcd for $C_{51}H_{87}N_3Si_4Zr$: C, 64.76; H, 9.27. Found: C, 64.84; H, 9.41.

$(Me_3SiCH_2)Zr[\eta^2$-C(CH_2SiMe_3)=NAr$]_2\{\eta^2$-C[Si(SiMe$_3$)$_3$]=NAr$\}$ (8). ArNC (0.052 g, 0.39 mmol) was added to **2** (0.078 g, 0.13 mmol) dissolved in toluene (2 mL) to give a bright yellow solution. The solution was then concentrated and slowly cooled to −18 °C to give 0.058 g of **8** as yellow crystals (45% yield). ^{1}H NMR (toluene-d_8, 400.1 MHz, 27 °C): δ 6.93 (m, 9H, C_6H_3), 2.61 (d, $^2J_{H-H}$ = 10.4 Hz, 2H, $NCCH_aH_bSiMe_3$), 2.57 (d, 2H, $NCCH_aH_bSiMe_3$) 2.08 (s, 6H, $C_6H_3Me_2$), 2.02 (s, 6H, $C_6H_3Me_2$), 2.01 (s, 6H, $C_6H_3Me_2$), 0.28 (s, 2H, $ZrCH_2SiMe_3$), 0.23 [s, 27H, Si(SiMe_3)$_3$], 0.02 (s, 9H, $ZrCH_2SiMe_3$), −0.10 (s, 18H, N=CCH_2-$SiMe_3$). ^{13}C{^{1}H} NMR (toluene-d_8, 100.6 MHz, 27 °C): δ 294.8 [N=CSi(SiMe$_3$)$_3$], 258.5 (N=CCH_2SiMe_3), 155.8, 149.4, 129.5, 128.9, 128.4, 128.1, 125.5, 125.2 (C_6H_3), 42.1 ($ZrCH_2SiMe_3$), 33.6 (N=CCH_2SiMe_3), 20.4 ($C_6H_3Me_2$), 20.3 ($C_6H_3Me_2$), 3.9

(9) (a) Casty, G. L.; Tilley, T. D.; Yap, G. P. A.; Rheingold, A. L. *Organometallics* **1997**, *16*, 4746. (b) Arnold, J.; Tilley, T. D.; Rheingold, A. L.; Geib, S. J.; Arif, A. M. *J. Am. Chem. Soc.* **1989**, *111*, 149. (c) Campion, B. K.; Heyn, R. H.; Tilley, T. D. *Organometallics* **1993**, *12*, 2584. (d) Honda, T.; Satoh, S.; Mori, M. *Organometallics* **1995**, *14*, 1548.

(10) Chiu, K. W.; Jones, R. A.; Wilkinson, G.; Galas, A. M. R.; Hursthouse, M. B. *J. Chem. Soc., Dalton Trans.* **1981**, 2088.

(11) Chamberlain, L. R.; Durfee, L. D.; Fanwick, P. E.; Kobriger, L.; Latesky, S. L.; McMullen, A. K.; Rothwell, I. P.; Folting, K.; Huffman, J. C.; Streib, W. E.; Wang, R. *J. Am. Chem. Soc.* **1987**, *109*, 390.

(12) Chamberlain, L. R.; Durfee, L. D.; Fanwick, P. E.; Kobriger, L.; Latesky, S. L.; McMullen, A. K.; Rothwell, I. P.; Folting, K.; Huffman, J. C.; Streib, W. E. *J. Am. Chem. Soc.* **1987**, *109*, 6068.

(13) Kloppenburg, L.; Petersen, J. L. *Organometallics* **1997**, *16*, 3548.

(14) Scott, M. J.; Lippard, S. J. *Organometallics* **1997**, *16*, 5857.

(15) Giannini, L.; Caselli, A.; Solari, E.; Floriani, C.; Chiesi-Villa, A.; Rizzoli, C.; Re, N.; Sgmellotti, A. *J. Am. Chem. Soc.* **1997**, *119*, 9709.

(16) See refs 3e and Dormond, A.; Aaliti, A.; Moise, C. *J. Chem. Soc., Chem. Commun.* **1985**, 1231.

Table 1. Crystallographic Data for 1, 3, and 7

	1	3	7
empirical formula	$C_{24}H_{60}Si_4Zr$	$C_{33}H_{69}NSi_4Zr$	$C_{51}H_{87}N_3Si_4Zr$
cryst size, mm	0.32 × 0.20 × 0.10	0.20 × 0.40 × 0.45	0.56 × 0.38 × 0.16
T, K	173(2)	173(2)	173(2)
cryst syst	trigonal	triclinic	triclinic
space group	*P*3	$P\bar{1}$	$P\bar{1}$
a, Å	16.282(4)	12.032(3)	11.557(3)
b, Å	16.282(4)	13.455(4)	14.462(5)
c, Å	11.608(4)	14.133(4)	17.228(5)
α, deg	90	111.99(2)	88.54(2)
β, deg	90	92.60(2)	89.13(2)
γ, deg	120	93.97(2)	72.95(2)
volume, Å^3	2665.0(13)	2110.2(10)	2752.0(14)
Z	3	2	2
fw	552.3	683.5	945.82
d_{calc}, g/cm^3	1.032	1.076	1.141
μ, mm^{-1}	0.453	0.394	0.320
F(000)	900	740	1020
scan type	$\omega-2\theta$	$\omega-2\theta$	$\omega-2\theta$
θ range,deg	2.27−22.55	1.56−22.55	1.84−22.55
no. of data [$I > 2\sigma(I)$]	2654	5527	7236
abs corr	semiempirical	semiempirical	semiempirical
R1[a] (wR2)[b]	0.0884 (0.1657)	0.0409 (0.0948)	0.0523 (0.1377)
GOF	1.082	1.105	1.117
no. of variables	263	376	532
$\rho_{max,min}$ (e Å^{-3})	0.589, −0.978	0.528, −0.383	0.828, −0.535

[a] $R1 = \sum||F_o| - |F_c||/\sum|F_o|$. [b] $wR2 = (\sum[w(F_o^2 - F_c^2)^2]/\sum[w(F_o^2)^2)^{1/2}$.

($ZrCH_2SiMe_3$), 3.1 [$Si(SiMe_3)_3$], 0.6 ($N{=}CCH_2SiMe_3$). ^{1}H NMR (toluene-d_8, 400.1 MHz, 52 °C): δ 6.95 (m, 9H, C_6H_3), 2.58 (s, 4H, $N{=}CCH_2SiMe_3$), 2.09 (s, 6H, $C_6H_3Me_2$), 2.01(s, 12H, $C_6H_3Me_2$), 0.28 (s, 2H, $ZrCH_2SiMe_3$), 0.23 [s, 27H, $Si(SiMe_3)_3$], 0.02 (s, 9H, $ZrCH_2SiMe_3$), −0.10 (s, 18H, $N{=}CCH_2SiMe_3$). $^{13}C\{^1H\}$ NMR (toluene-d_8, 100.6 MHz, 52 °C): δ 295.3 [$N{=}CSi(SiMe_3)_3$], 258.9 ($N{=}CCH_2SiMe_3$), 155.8, 149.6, 129.5, 128.9, 128.4, 128.1, 125.5, 125.2 (C_6H_3), 42.5 ($ZrCH_2SiMe_3$), 33.8 ($N{=}CCH_2SiMe_3$), 20.4 ($C_6H_3Me_2$), 20.3 ($C_6H_3Me_2$), 3.9 ($ZrCH_2SiMe_3$), 3.2 [$Si(SiMe_3)_3$], 0.7 ($N{=}CCH_2SiMe_3$). Anal. Calcd for $C_{48}H_{87}N_3Si_7Zr$: C, 58.00; H, 8.82. Found: C, 57.77; H, 9.10.

X-ray Data Collection and Structural Analyses of 1, 3, and 7. All crystal structures were determined on a Siemens R3m/V diffractometer equipped with a Nicolet LT-2 low-temperature device. Suitable crystals were coated with Paratone oil (Exxon) and mounted under a stream of nitrogen at −100 °C. The unit cell parameters and orientation matrix were determined from a least-squares fit of the orientation of at least 25 reflections obtained from a rotation photograph and an automatic peak search routine. The refined lattice parameters and other pertinent crystallographic information are given in Table 1.

Intensity data were measured with graphite-monochromated Mo Kα radiation (λ = 0.710 73 Å). Background counts were measured at the beginning and end of each scan with the crystal and counter kept stationary. The intensities of three standard reflections were measured after every 97 reflections. The intensity data were corrected for Lorentz and polarization effects and an empirical absorption correction based upon ψ scans.

The structures were solved using the Siemens SHELXTL 93 (version 5.0) proprietary software package. For **7**, the zirconium and silicon atoms were located by the Patterson method, and the structure completed by successive Fourier syntheses. For **1** and **3**, the structures were solved by direct methods. All non-hydrogen atoms were refined anisotropically. The α-hydrogen atoms of the neopentyl ligands in **3** were located from a Fourier difference map and refined isotropically. The remaining hydrogen atoms in **3** and those in **1** and **7** were placed in calculated positions and introduced into the refinement as fixed contributors with an isotropic *U* value of 0.08 Å^2.

Scheme 2

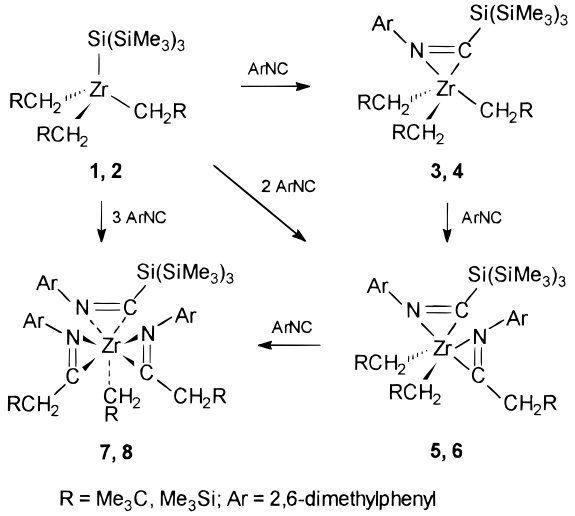

Results and Discussion

Synthesis and Characterization of ArNC Insertion Products 3−8. The alkyl silyl complexes **1** and **2** react with 1 equiv of ArNC instantaneously at room temperature to produce the *silyl* insertion products $(Me_3ECH_2)_3Zr\{\eta^2\text{-}C[Si(SiMe_3)_3]{=}NAr\}$ [E = C (**3**), Si (**4**)]. The mono-insertion products **3** and **4** are highly soluble in pentane and hexanes, and were purified by recrystallization from toluene. **3** and **4** are stable under nitrogen at room temperature. When 2 equiv of ArNC were added to **1** and **2**, di-insertion intermediates $(Me_3ECH_2)_2Zr[\eta^2\text{-}C(CH_2EMe_3){=}NAr]\{\eta^2\text{-}C[Si(SiMe_3)_3]{=}NAr\}$ [E = C (**5**), Si (**6**)] were clearly identifiable by NMR (Scheme 2). However, attempts to isolate pure products were unsuccessful; small amounts of tri-insertion products were present in the isolated materials.[17] The tri-insertion complexes $(Me_3ECH_2)Zr[\eta^2\text{-}C(CH_2EMe_3){=}NAr]_2\{\eta^2\text{-}C[Si(SiMe_3)_3]{=}NAr\}$ [E = C (**7**), Si (**8**)] were obtained by either the reactions of 3 equiv of ArNC with **1** and **2**, or addition of 2 equiv of ArNC to **3** and **4**

Table 2. Selected ^{13}C NMR Data[a]

complexes	δ(N=*C*R)	δ(N=*C*Si)	δ[Si(Si*Me*$_3$)$_3$]
$Np_3ZrSi(SiMe_3)_3$ (**1**)[7b]			4.2
$Ns_3ZrSi(SiMe_3)_3$ (**2**)[7b]			4.3
$Np_3Zr\{\eta^2$-C[Si(SiMe$_3$)$_3$]=NAr$\}$ (**3**)		296.0	2.6
$Ns_3Zr\{\eta^2$-C[Si(SiMe$_3$)$_3$]=NAr$\}$ (**4**)		297.5	2.4
$Np_2Zr[\eta^2$-C(Np)=NAr$]\{\eta^2$-C[Si(SiMe$_3$)$_3$]=NAr$\}$ (**5**)	259.9	295.5	2.9
$Ns_2Zr[\eta^2$-C(Ns)=NAr$]\{\eta^2$-C[Si(SiMe$_3$)$_3$]=NAr$\}$ (**6**)	257.7	297.5	2.6
$NpZr[\eta^2$-C(Np)=NAr$]_2\{\eta^2$-C[Si(SiMe$_3$)$_3$]=NAr$\}$ (**7**)	261.0	298.8	3.5
$NsZr[\eta^2$-C(Ns)=NAr$]_2\{\eta^2$-C[Si(SiMe$_3$)$_3$]=NAr$\}$ (**8**)	258.5	294.8	3.1
$Cp_2Sc\{\eta^2$-C[Si(SiMe$_3$)$_3$]=NAr$\}$[11c]		299.07	2.89
$Cp_2Zr\{\eta^2$-C[Si(SiMe$_3$)$_3$]=NAr$\}$Cl[3b]		267.6	3.30
CpCp*Zr$\{\eta^2$-C[Si(SiMe$_3$)$_3$]=NAr$\}$Cl[3e]		272.40	4.24
(Bu^{t}O)$_3$Zr$\{\eta^2$-C[Si(SiMe$_3$)$_3$]=NAr$\}$[3f]		299.01	2.24
Cp′Zr$[\eta^2$-C(Me)=NAr$]_2$[13]	251.8		
(2,6-Bu$^t_2$C$_6$H$_3$O)$_2$Zr$[\eta^2$-C(CH$_2$Ph)=NAr$]$(CH$_2$Ph)[11]	246.3		
(2,6-Bu$^t_2$C$_6$H$_3$O)$_2$Zr$[\eta^2$-C(Me)=NAr$]_2$[11]	245.2		

[a] R = alkyl; Np = Me_3CCH_2; Ns = Me_3SiCH_2; Cp′ = $(C_5Me_4)SiMe_2(NBu^t)$.

(Scheme 2). **7** and **8**, highly soluble in pentane and hexane, have a lower solubility in toluene, and were thus purified by recrystallization from toluene. The 14-electron complexes **7** and **8** are inert to further reaction with ArNC and were found to be more stable toward oxidation in air than their 8-electron precursors **1** and **2**.

All insertion products have been characterized by ^1H and ^{13}C NMR spectroscopy. The NMR spectra of the mono-insertion complexes **3** and **4** revealed that the ^1H and ^{13}C resonances of the Si(SiMe$_3$)$_3$ group in **3** and **4** are both upfield-shifted compared to those of their alkyl silyl precursors. The characteristic η^2-iminosilaacyl carbon resonances for **3** and **4** at 296.0 and 297.5 ppm, respectively, are similar to those in other η^2-iminosilaacyl complexes (Table 2) and suggest that the first ArNC inserts into the Zr−Si bonds in **1** and **2**. The ^1H NMR spectra of the tri-insertion products **7** and **8** at 206 K show a singlet for the α-protons of the non-inserted Zr−C*H*$_2$CMe$_3$ and Zr−C*H*$_2$SiMe$_3$ ligands as well as an AB pattern for the methylene protons of the inserted −C*H*$_2$CMe$_3$ and −C*H*$_2$SiMe$_3$ groups. The AB pattern in the ^1H NMR of **8** is shown in Figure 1. This AB pattern suggests two motions in **7** and **8**. First, there is a facile rotation (flipping) of the η^2-iminosilaacyl ligand, which makes the two η^2-iminoacyl groups chemically equivalent (Chart 1a). Second, the rotation of the two η^2-iminoacyl ligands (Chart 1b) is fast on the NMR time scale, which, combined with the rotation of the η^2-iminosilaacyl group, gives rise to one set of diastereotopic methylene protons for the η^2-iminoacyl ligands in **7** and **8**. The AB pattern in the ^1H NMR of **7** and **8** is also consistent with static η^2-iminoacyl groups (no rotation with respect to the Zr centers). Although this possibility is unlikely, we cannot currently rule it out.

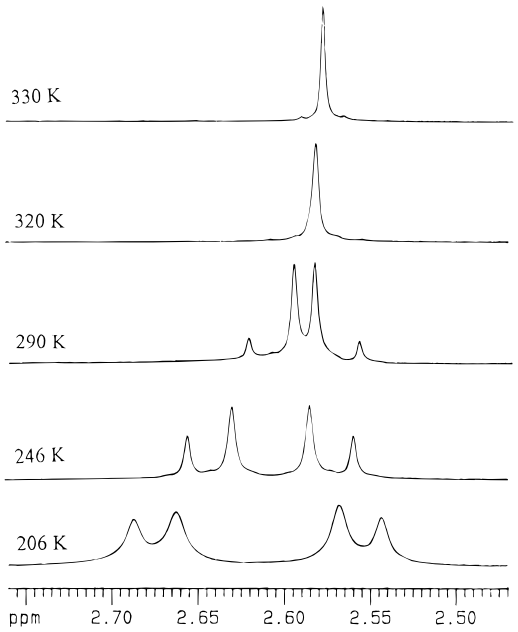

Figure 1. Variable-temperature NMR spectra of (Me$_3$SiCH$_2$)Zr$(\eta^2$-C(CH$_2$SiMe$_3$)=NAr$)_2\{\eta^2$-C[Si(SiMe$_3$)$_3$]=NAr$\}$ (**8**).

The variable-temperature ^1H NMR of **7** and **8** has been studied. The diastereotopic methylene proton resonances of the η^2-iminoacyl ligands in **8** coalesce to one single peak at 320 K (Figure 1). The free energy of activation $\Delta G^{\ddagger}$ for the coalescence at 320 K was estimated to be 15.7 ± 0.5 kcal/mol.[18] This phenomenon suggests another dynamic process in **8**, namely an exchange between two η^2-iminoacyl ligands (Chart 1c), which equilibrates their diastereotopic methylene protons. A similar ligand exchange in (2,6-Bu$^t_2$C$_6$H$_3$O)Zr$[\eta^2$-C(CH$_2$Ph)=NAr$]_2$(CH$_2$Ph) has been reported by Rothwell and co-workers.[11] The AB pattern in the ^1H NMR spectra of **7** remains unchanged between 206 and 330 K. This suggests a high degree of steric congestion in **7** compared to that in **8**, restricting the ligand-exchange between the two η^2-iminoacyl ligands in **7**. The CH$_2$-

(17) NMR data for the di-insertion complex $(Me_3CCH_2)_2Zr[\eta^2$-C(CH$_2$CMe$_3$)=NAr$]\{\eta^2$-C[Si(SiMe$_3$)$_3$]=NAr$\}$ (**5**): ^1H NMR (benzene-d_6, 250 MHz, 23 °C): δ 7.02, 6.95 (m, 6H, C$_6H_3$), 2.48 (s, 2H, N=CC*H*$_2$CMe$_3$), 2.19 (s, 6H, C$_6$H$_3$*Me*$_2$), 2.16 (s, 6H, C$_6$H$_3$*Me*$_2$), 1.13 (s, 18H, ZrCH$_2$C*Me*$_3$), 0.95 (s, 4H, ZrC*H*$_2$CMe$_3$), 0.89 (s, 9H, N=CCH$_2$C*Me*$_3$), 0.24 [s, 27H, Si(Si*Me*$_3$)$_3$]. $^{13}C\{^1H\}$ NMR (benzene-d_6, 62.9 MHz, 23 °C): δ 295.5 [N=*C*Si(SiMe$_3$)$_3$], 259.9 (N=*C*CH$_2$CMe$_3$), 156.4, 150.1, 129.1, 128.7, 128.2, 127.6, 125.9, 125.7 (*C*$_6$H$_3$), 88.9 (ZrCH$_2$CMe$_3$), 52.2 (N=CCH$_2$CMe$_3$), 36.1 (ZrCH$_2$*C*Me$_3$), 35.1 (ZrCH$_2$C*Me*$_3$), 31.9 (N=CCH$_2$*C*Me$_3$), 30.7 (N=CCH$_2$C*Me*$_3$), 20.1 (C$_6$H$_3$*Me*$_2$), 19.8 (C$_6$H$_3$*Me*$_2$), 2.9 [Si(Si*Me*$_3$)$_3$]. NMR data for the di-insertion complex $(Me_3SiCH_2)_2Zr[\eta^2$-C(CH$_2$SiMe$_3$)=NAr$]\{\eta^2$-C[Si(SiMe$_3$)$_3$]=NAr$\}$ (**6**): ^1H NMR (benzene-d_6, 250 MHz, 23 °C): δ 7.04−6.97 (m, 6H, C$_6H_3$), 2.78 (s, 2H, N=CC*H*$_2$SiMe$_3$), 2.28 (s, 6H, C$_6$H$_3$*Me*$_2$), 2.19 (s, 6H, C$_6$H$_3$*Me*$_2$), 0.37 (s, 2H, ZrC*H*$_2$SiMe$_3$), 0.34 (s, 2H, ZrC*H*$_2$SiMe$_3$), 0.21 [s, 27H, Si(Si*Me*$_3$)$_3$] 0.07 (s, 18H, ZrCH$_2$Si*Me*$_3$), −0.06 (s, 9H, N=CCH$_2$Si*Me*$_3$). $^{13}C\{^1H\}$ NMR (benzene-d_6, 62.9 MHz, 23 °C): δ 297.5 [N=*C*Si(SiMe$_3$)$_3$], 257.7 (N=*C*CH$_2$SiMe$_3$), 156.0, 148.9, 129.1, 128.8, 127.8, 127.0, 126.0, 125.8 (*C*$_6$H$_3$), 56.8 (ZrCH$_2$SiMe$_3$), 34.2 (N=CCH$_2$SiMe$_3$), 20.3 (C$_6$H$_3$*Me*$_2$), 19.9 (C$_6$H$_3$*Me*$_2$), 3.3 (ZrCH$_2$Si*Me*$_3$), 2.6 [Si(Si*Me*$_3$)$_3$], 0.15 (N=CCH$_2$Si*Me*$_3$).

(18) For the evaluation of exchange rate constants from the AB case in NMR spectra, see: Sandstrom, J. *Dynamic NMR Spectroscopy*; Academic Press: New York, 1982; p 84.

Chart 1

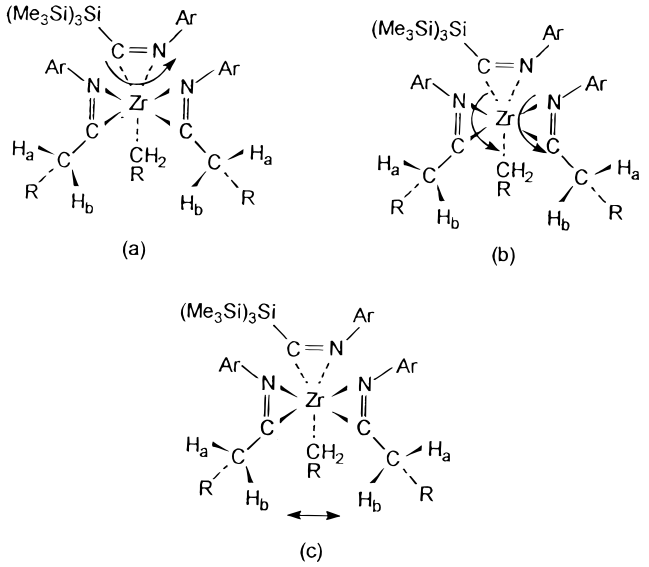

CMe_3 groups in **7** are more sterically demanding than the CH_2SiMe_3 groups in **8** [the C−Si bond (ca.1.85 Å) is longer than the C−C bond (ca. 1.54 Å)] and thus contribute significantly to the steric congestion in **7**.[19]

Molecular Structure of $(Me_3CCH_2)_3ZrSi(SiMe_3)_3$ (1). The structure of **1**, the precursor to **3** and **7**, was determined in part to compare it with those of **3** and **7**. An ORTEP drawing of **1** is shown in Figure 2. There are three unique but chemically equivalent molecules in a unit cell, and only one representative molecule is shown. Selected bond distances and angles are listed in Table 3. As expected, the structure of **1** is analogous to that of its titanium analogue $(Me_3CCH_2)_3TiSi(SiMe_3)_3$.[7b] The crystal structure reveals a 3-fold axis of symmetry along the M−Si bond. The alkyl groups on the Zr metal are staggered with respect to the trimethylsilyl groups on the central silicon atom. The three alkyl and the silyl ligands are arranged in a pseudotetrahedral geometry around the metal center, giving a formally 8-electron species. The angles (C−Zr−C) between the alkyl ligands are 113.0(7)° (mean). The angles (C−Zr−Si) between the alkyl and silyl ligands are 105.6(8)°. These angles are close to those found in $(Me_3CCH_2)_3TiSi(SiMe_3)_3$ and $(Me_3SiCH_2)_3TiSi(SiMe_3)_3$.[7b] The C−Zr−C angles in **1** are wider than the C−Zr−Si angles and may indicate that the steric interaction among the alkyl ligands is greater than that between alkyl and silyl ligands. The greater Zr−Si bond and Si−Si distances apparently make the central silicon atom in the $Si(SiMe_3)_3$ group relatively uncrowed; the bonding about the central silicon atom is not greatly distorted from tetrahedral [the mean Zr−Si−Si angle: 110.9(5)°]. In contrast, the shorter Zr−C bonds and bulky Me_3C groups on three Me_3CCH_2 ligands contribute to the steric strain among these ligands, and perhaps force the widening of the Zr−C−C angles [av 137(2)°]. No α-agostic interactions are observed in either the solid-state structure or solution NMR of **1**, which often occurs in electron deficient early-transition-metal alkyl complexes.[20]

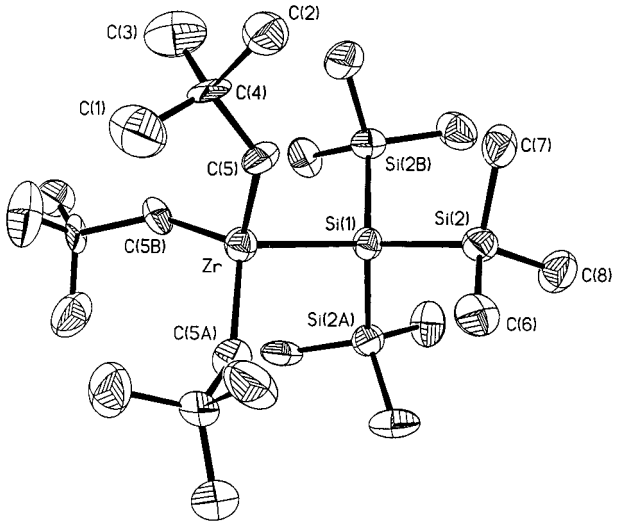

Figure 2. ORTEP drawing of $(Me_3CCH_2)_3ZrSi(SiMe_3)_3$ (**1**), showing 50% thermal ellipsoids.

Table 3. Selected Bond Distances (Å) and Angles (deg) for 1

		Distances	
Zr−Si(1)	2.74(2)	Si(1)−Si(2)	2.345(12)
Zr−C(5)	2.11(3)	Si(1′)-Si(2′)	2.347(13)
Zr′-Si(1′)	2.72(2)	Si(1″)−Si(2″)	2.320(9)
Zr′−C(5′)	2.09(3)	C(4)−C(5)	1.55(3)
Zr″−Si(1″)	2.76(2)	C(4′)-C(5′)	1.55(4)
Zr″−C(5″)	2.14(3)	C(4")-C(5")	1.53(4)
		Angles	
Si(1)−Zr−C(5)	104.5(8)	C(5)−Zr−C(5A)	113.9(6)
Si(1′)−Zr′−C(5′)	105.9(10)	C(5′)−Zr′−C(5′A)	112.8(8)
Si(1″)−Zr″−C(5″)	106.4(7)	C(5″)−Zr″−C(5″A)	112.3(7)
Zr−Si(1)−Si(2)	110.7(5)	Si(2)−Si(1)−Si(2A)	108.2(5)
Zr′−Si(1′)−Si(2′)	111.3(5)	Si(2′)−Si(1′)−Si(2′A)	107.5(6)
Zr″−Si(1″)−Si(2″)	110.7(4)	Si(2″)−Si(1″)−Si(2″A)	108.2(4)
Zr−C(5)−C(4)	138(2)	Zr′−C(5′)−C(4′)	136(3)
Zr″−C(5″)−C(4″)	138(2)		

The mean Zr−C bond distance of 2.11(2) Å in **1** is slightly shorter than those found in some more electron-rich Zr(IV) neopentyl complexes, such as $Cp_2Zr(CH_2CMe_3)_2$ [2.294(8) Å],[19] $[(Me_3CCH_2)_3ZrCl]_n$ [2.200(4) Å],[21] $(F_6\text{-acen})Zr(CH_2CMe_3)_2$ [2.283(4) and 2.323(5) Å], and $[(F_6\text{-acen})Zr(CH_2CMe_3)(NMe_2Ph)][B(C_6F_5)_4]$ [2.175(5) Å].[22] The mean Zr−Si bond distance of 2.74(2) Å is close to those in $(Bu^tO)_3ZrSi(SiMe_3)_3$ [2.753(4) Å],[3f] $Cp_2Zr[Si(SnMe_3)_3]Cl$ [2.772(4) Å],[1b] and $Cp_2Zr(SiPh_3)(H)(PMe_3)$ [2.721(2) Å][23] but is shorter than those in $(Me_3SiO)_2Zr(SiPh_2Bu^t)Cl(THF)_2$ [2.848(3) Å],[24] $Cp_2Zr(SiPh_3)Cl$ [2.813(2) Å],[25] and $Cp_2Zr(SiMe_3)(S_2CNEt_2)$ (2.815 Å).[26]

Molecular Structure of $(Me_3CCH_2)_3Zr\{\eta^2\text{-}C[Si(SiMe_3)_3]{=}NAr\}$ (3). The insertion of the first ArNC into Zr−Si bond in $(Me_3CCH_2)_3ZrSi(SiMe_3)_3$ (**1**) was confirmed by the X-ray crystal structure of **3**. An

(19) Jeffery, J.; Lappert, M. F.; Luong-Thi, N. T.; Webb, M. *J. Chem. Soc., Dalton Trans.* **1981**, 1593.

(20) (a) Brookhart, M.; Green, M. L. H.; Wong, L. *Prog. Inorg. Chem.* **1988**, *36*, 1. (b) Crabtree, R. H.; Hamilton, D. G. *Adv. Organomet. Chem.* **1988**, *28*, 299. (c) Grubbs, R. H.; Coates, G. W. *Acc. Chem. Res.* **1996**, *29*, 85.

(21) (a) Hoyt, L. K.; Pollitte, J. L.; Xue, Z. *Inorg. Chem.* **1994**, *33*, 2497. (b) McAlexander, L. H.; Li, L.; Yang, Y.; Pollitte, J. L.; Xue, Z. *Inorg. Chem.* **1998**, *37*, 1423.

(22) Tjaden, E. B.; Swenson, D. C.; Jordan, R. F.; Petersen, J. L. *Organometallics* **1995**, *14*, 371.

(23) Kreutzer, K. A.; Fisher, R. A.; Davis, W. M.; Spaltenstein, E.; Buchwald, S. L. *Organometallics* **1991**, *10*, 4031.

(24) Wu, Z., Diminnie, J. B.; Xue, Z. *Organometallics* **1998**, *17*, 2917.

(25) Muir, K. *J. Chem. Soc. A* **1971**, 2663.

(26) Tilley, T. D. *Organometallics* **1985**, *4*, 1452.

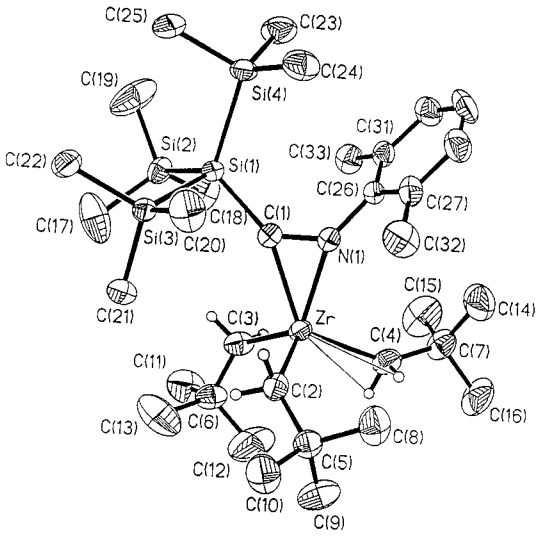

Figure 3. ORTEP drawing of $(Me_3CCH_2)_3Zr\{\eta^2\text{-}C[Si(SiMe_3)_3]{=}NAr\}$ (**3**), showing 50% thermal ellipsoids.

Table 4. Selected Bond Distances (Å) and Angles (deg) for 3

		Distances	
Zr−C(1)	2.255(4)	C(1)−N(1)	1.293(5)
Zr−C(2)	2.237(5)	C(1)−Si(1)	1.897(4)
Zr−C(3)	2.256(5)	Si(1)−Si(2)	2.365(2)
Zr−C(4)	2.213(5)	Si(1)−Si(3)	2.361(2)
Zr−N(1)	2.175(3)	Si(1)−Si(4)	2.368(2)
Zr−H(4A)	2.40(5)	Zr−H(4B)	2.42(5)
		Angles	
C(1)−Zr−C(2)	108.5(2)	Zr−C(1)−Si(1)	156.5(2)
C(1)−Zr−C(3)	93.7(2)	Zr−N(1)−C(26)	154.0(3)
C(1)−Zr−C(4)	128.0(2)	Zr−C(2)−C(5)	134.7(3)
C(2)−Zr−C(3)	114.0(2)	Zr−C(3)−C(6)	130.1(3)
C(2)−Zr−C(4)	108.3(2)	Zr−C(4)−C(7)	145.9(3)
C(3)−Zr−C(4)	103.3(2)	Zr−C(1)−N(1)	69.7(2)
C(2)−Zr−N(1)	114.1(2)	C(1)−Zr−N(1)	33.87(13)
C(4)−Zr−N(1)	96.9(2)	C(3)−Zr−N(1)	117.6(2)
Zr−C(4)−H(4A)	90(3)	Zr−C(4)−H(4B)	92(3)

ORTEP drawing of complex **3** is shown in Figure 3. Selected bond distances and angles are listed in Table 4. The zirconium atom is coordinated by one η^2-iminosilaacyl and three CH_2CMe_3 ligands, giving a formally 10-electron species. The geometry around the metal atom can be best described as a pseudotetrahedron with an η^2-N=C unit occupying a single coordination site. The ZrCN unit and one CH_2CMe_3 ligand closely lie in one plane with an alkyl ligand on each side of the plane. One of the three alkyl ligands [$C(4)H_2CMe_3$] points toward the iminosilaacyl ligand while the other two point away from it. In comparison, in the structure of the precursor **1**, all three CH_2CMe_3 ligands point away from the bulky $Si(SiMe_3)_3$ ligand. The complex **3** is perhaps sterically less crowded than **1**, allowing the neopentyl ligands to adopt a different orientation.

It is interesting to note that the α-C angles in the Zr−alkyl ligands in **3** are 130.2(3), 134.5(3), and 145.9(3)°. The first two angles are slightly smaller than that in **1** [av 137(2)°]; the other one significantly differs from the first two and is about 8° larger than that in **1**. The reason for this large Zr−C−C angle may be due to agostic interactions between the metal center and the α-protons of the neopentyl methylene. Two hydrogen atoms on the $C(4)H_2CMe_3$ ligand lie in close contact (av 2.41 Å) with the metal center giving rise to Zr−C−Hα angles of 90 and 92° (see Figure 3). The methylene protons of the three neopentyl ligands were located from a difference map and refined isotropically. The $Zr-H_{4a}$ and $Zr-H_{4b}$ bond distances are 2.40(5) and 2.42(5) Å, respectively, which are comparable to those in the related early-transition-metal alkyl complexes, such as $CpNb(=N\text{-}2,6\text{-}C_6H_3\text{-}Pr^i_2)(CH_2CMe_3)_2$ (Pr^i = Me_2CH) [2.321(29) and 2.405(33) Å],[27] $(dmpe)Zr(CH_2SiMe_3)_4$ (2.48 Å),[28] $Cp^*Ti(CH_2Ph)_3$ (2.32 and 2.37 Å),[29] $Tp^*NbCl(CH_2SiMe_3)(PhC{\equiv}CMe)$ [2.29(6) Å],[30] and $Cp_2Th(CH_2CMe_3)_2$ [2.597(9) and 2.648(9) Å],[31] when the difference in metal ion radii is taken into account. The Zr−C(4) distance of 2.213(5) Å is slightly shorter than the other two Zr−C(alkyl) bonds in **3** [2.237(5) and 2.256(5) Å] and is very close to that in $(dmpe)Zr(CH_2SiMe_3)_4$ [2.215(9) Å].[26] The infrared spectrum of **3** showed a medium-strong band at 2790 cm^{-1} and a weak absorption at 2700 cm^{-1}, which can be attributed to agostic C−H stretches in **3**.[20,32,33]

No evidence of an agostic interaction between the metal center and α-protons of neopentyl ligands is seen in the solution NMR of **3**. From the solid-state structure, one would expect the NMR spectra of **3** to show two sets of *tert*-butyl signals from the CH_2CMe_3 ligands in a 2:1 ratio. However, only one set of neopentyl resonances were observed in the variable-temperature NMR spectra of **3** (193−300 K), indicating either a free rotation of the iminosilaacyl ligand or a rapid exchange of the three CH_2CMe_3 ligands in **3** in solution.

The Zr−C(alkyl) bond distances range from 2.213(5) to 2.257(5) Å and are slightly longer than that in **1** [2.11(3) Å]. The Zr−C(1) [2.255(4) Å] and Zr−N(1) [2.175(3) Å] bond distances are slightly shorter than those in $Cp_2Zr[\eta^2\text{-}C(NPh)SiPhBu^t]Cl$ (2.28 and 2.19 Å)[9d] and $CpCp^*Zr[\eta^2\text{-}C(NAr)Si(SiMe_3)_3]Cl$ [2.309(10) and 2.249(8) Å].[3e] The angles within the ZrCN unit are similar to those in other Zr iminoacyl and iminosilaacyl complexes.[3e,9d,11,13,15]

Molecular Structure of $(Me_3CCH_2)Zr[\eta^2\text{-}C(CH_2CMe_3){=}NAr]_2\{\eta^2\text{-}C[Si(SiMe_3)_3]{=}NAr\}$ (7). An ORTEP drawing of **7** is shown in Figure 4. Selected bond distances and angles are given in Table 5. The zirconium atom is bonded to one η^2-iminosilaacyl, one neopentyl, and two η^2-iminoacyl ligands to form a seven-coordinate metal complex. However, an analysis of the calculated centroids of the C=N bonds shows that the coordination sphere about the zirconium center is pseudo-tetrahedral. This coordination sphere, as shown in the simplified view in Figure 5, is different from that observed in a tris(η^2-iminoacyl) complex $(2,6\text{-}Bu^t_2C_6H_3O)Zr[\eta^2\text{-}C(CH_2Ph){=}NAr]_3$,[11] where two iminoacyl groups are coplanar. Larger steric repulsion is expected in **7**, which contains bulky $Si(SiMe_3)_3$ and neopentyl groups. The C=N

(27) Poole, A. D.; Williams, D. N.; Kenwright, A. M.; Gibson, V. C.; Clegg, W.; Hockless, D. C. R.; O'Neil, P. A. *Organometallics* **1993**, *12*, 2549.
(28) Cayias, J. Z.; Babaian, E. A.; Hrncir, D. C.; Bott, S. G.; Atwood, J. L. *J. Chem. Soc., Dalton Trans.* **1986**, 2743.
(29) Mena, M.; Pellinghelli, M. A.; Royo, P.; Serrano, R.; Tiripicchio, A. *J. Chem. Soc., Chem. Commun.* **1986**, 1118.
(30) Etienne, M.; Mathieu, R.; Donnadieu, B. *J. Am. Chem. Soc.* **1997**, *119*, 3218.
(31) Bruno, J. W.; Smith, G. M.; Marks, W. J.; Fair, C. K.; Schultz, A. J.; Williams, J. M. *J. Am. Chem. Soc.* **1986**, *108*, 40.
(32) Morse, P. M.; Spencer, M. D.; Wilson, S. R.; Girolami, G. S. *Organometallics* **1994**, *13*, 1646.
(33) McGrady, G. S.; Downs, A. J.; Hamblin, J. M. *Organometallics* **1995**, *14*, 3738.

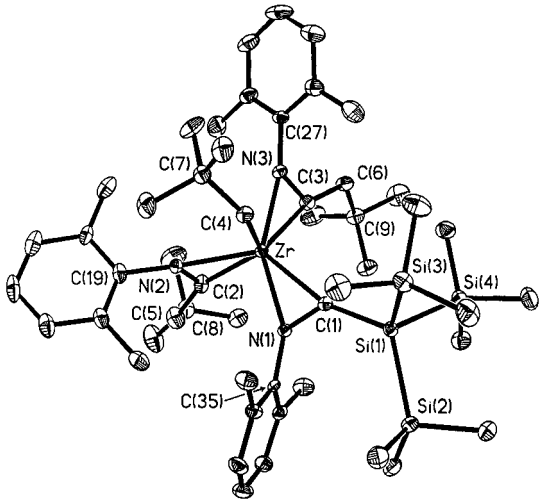

Figure 4. ORTEP drawing of $(Me_3CCH_2)Zr(\eta^2\text{-}C(CH_2CMe_3)=NAr)_2\{\eta^2\text{-}C[Si(SiMe_3)_3]=NAr\}$ (**7**), showing 35% thermal ellipsoids.

Table 5. Selected Bond Distances (Å) and Angles (deg) for 7

		Distances	
Zr−C(1)	2.319(5)	C(1)−N(1)	1.283(6)
Zr−C(2)	2.301(5)	C(2)−N(2)	1.273(6)
Zr−C(3)	2.265(5)	C(3)−N(3)	1.283(6)
Zr−C(4)	2.301(5)	C(1)−Si(1)	1.921(5)
Zr−N(1)	2.200(4)	Si(1)−Si(2)	2.380(2)
Zr−N(2)	2.270(4)	Si(1)−Si(3)	2.369(2)
Zr−N(3)	2.242(4)	Si(1)−Si(4)	2.351(2)
N(1)−C(35)	1.433(6)	N(3)−C(27)	1.442(6)
N(2)−C(19)	1.454(6)	C(3)−C(6)	1.506(7)
C(2)−C(5)	1.536(7)	C(4)−C(7)	1.527(7)
		Angles	
Zr−C(1)−N(1)	68.5(3)	N(1)−Zr−N(2)	98.58(14)
Zr−C(1)−Si(1)	163.1(2)	N(1)−Zr−N(3)	152.34(14)
Zr−N(1)−C(1)	78.7(3)	N(1)−Zr−C(2)	90.5(2)
Zr−N(1)−C(35)	151.0(3)	N(1)−Zr−C(3)	124.2(2)
Zr−C(2)−N(2)	72.5(3)	N(1)−Zr−C(4)	98.1(2)
Zr−C(2)−C(5)	161.4(4)	N(2)−Zr−N(3)	107.93(14)
Zr−N(2)−C(2)	75.2(3)	N(2)−Zr−C(1)	130.1(2)
Zr−N(2)−C(19)	159.1(3)	N(2)−Zr−C(3)	120.3(2)
Zr−C(3)−N(3)	72.4(3)	N(2)−Zr−C(4)	93.3(2)
Zr−C(3)−C(6)	165.1(4)	N(3)−Zr−C(1)	121.9(2)
Zr−N(3)−C(3)	74.5(3)	N(3)−Zr−C(2)	107.7(2)
Zr−N(3)−C(27)	159.7(3)	N(3)−Zr−C(4)	88.3(2)
Zr−C(4)−C(7)	137.2(4)	C(1)−Zr−C(2)	121.7(2)
C(1)−Zr−C(3)	103.7(2)	C(1)−Zr−C(4)	86.7(2)
C(2)−Zr−C(3)	101.7(2)	C(2)−Zr−C(4)	125.5(2)
C(3)−Zr−C(4)	116.3(2)	C(1)−Zr−N(1)	32.8(2)
C(2)−Zr−N(2)	32.3(2)	C(3)−Zr−N(3)	33.1(2)

distances and the internal angles within the three-membered ZrCN rings are similar to those found in **3** and other zirconium η^2-iminoacyl and η^2-iminosilaacyl complexes.[3e,9d,11,13,15] The Zr−C(η^2-iminosilaacyl) bond [2.319(5) Å] is slightly longer than the Zr−C(η^2-iminoacyl) bonds [2.301(5) and 2.265(5) Å] (Table 5), perhaps due to the steric effect of the bulky η^2-iminosilaacyl ligand. In addition, the Zr−C(η^2-iminosilaacyl) [2.319(5) Å], Si−C(=N) [1.921(5) Å], and Zr−C(4) [2.301(5) Å] distances are longer than the corresponding values found in the mono-insertion complex **3** [2.255(4), 1.898(4), and 2.206(5)−2.255(5) Å, respectively]. These are consistent with more steric congestion in the tri-insertion complex **7**.

Preferential Isocyanide Insertion into Silyl−Zr Bonds. Tilley and co-workers[3e] have investigated the insertion of ArNC into CpCp*Zr[Si(SiMe$_3$)$_3$]Me (Cp* = η^5-C$_5$Me$_5$) and found that such insertion occurred exclusively to the Zr−Me bond to form an iminoacyl complex. In contrast, the first insertion of ArNC into Cp-free alkyl silyl complexes $(Me_3ECH_2)_3ZrSi(SiMe_3)_3$ [E = C (**1**), Si (**2**)] occurs to the M−Si bonds to give silyl insertion complexes **3** and **4**. To our knowledge, the mono-insertion complexes **3** and **4** represent the first example of isocyanide insertion into a M−Si bond in the presence of competing M−C bonds.

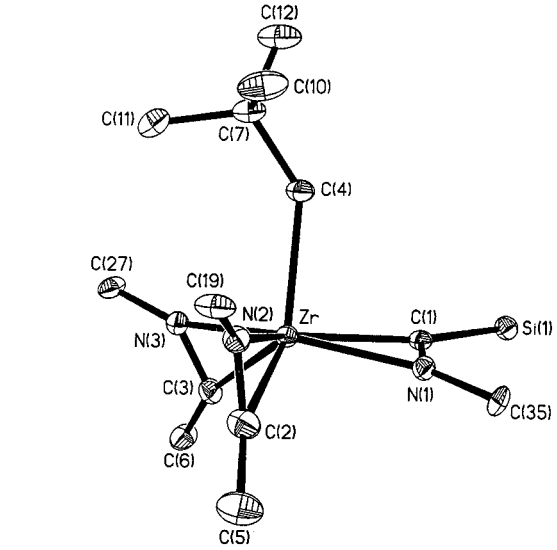

Figure 5. Simplified ORTEP drawing of the structure of $(Me_3CCH_2)Zr(\eta^2\text{-}C(CH_2CMe_3)=NAr)_2\{\eta^2\text{-}C[Si(SiMe_3)_3]=NAr\}$ (**7**).

Scheme 3. Proposed Mechanism of the First ArNC Insertion into the Zr−Si Bonds in 1 and 2

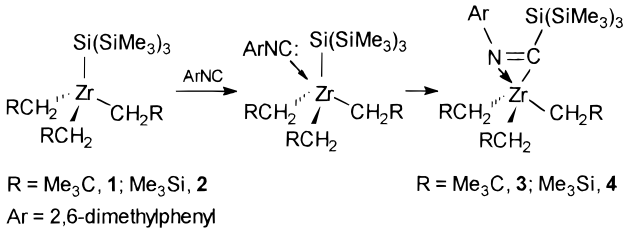

Tilley and co-workers also observed that CO preferentially inserts into the Zr−C bond in $Cp_2Zr(Me)Si(SiMe_3)_3$[3b] and, in contrast, into the Zr−Si bond in CpCp*Zr(Me)Si(SiMe$_3$)$_3$.[3e] In the current studies, insertion into the Zr−Si bonds is exclusive in the reactions of **1** and **2** with first ArNC. It is not fully understood what led to such exclusive insertion. The Zr−Si bonds are usually weaker than Zr−C bonds. The bond disruption enthalpy (BDE) for the Zr−Si(SiMe$_3$)$_3$ in $Cp_2Zr[Si(SiMe_3)_3]Cl$ (BDE = 56 kcal/mol)[34] is smaller than those of the Zr-alkyl bonds in $Zr(CH_2CMe_3)_4$ (BDE = 60 kcal/mol) and $Zr(CH_2SiMe_3)_4$ (BDE = 74 kcal/mol).[35] In addition, the Si(SiMe$_3$)$_3$ ligand is bulkier than CH_2CMe_3 and CH_2SiMe_3 ligands; insertion into Zr−Si bonds in **1** and **2** will likely relieve more steric strain than insertion into Zr−C bonds. The structures of **1** and **3** (Figures 2 and 3) reveal that the average C−Zr−C angle in **1** (113°) is larger than that in the insertion product **3** (108.5°), indicating that the steric repulsion between the three

(34) King, W. A.; Marks, T. J. *Inorg. Chim. Acta* **1995**, *229*, 343.
(35) Lappert, M. F.; Patil, D. S.; Pedley, J. B. *J. Chem. Soc., Chem. Commun.* **1975**, 830.

CH_2CMe_3 ligands in **3** decreases compared to that in **1**. These analyses indicate that the silyl migratory insertion in **1** and **2** is favorable. In addition, the results suggest that the first isocyanide adds between the alkyl and silyl ligands (cis to the silyl ligand), as shown in the proposed mechanism in Scheme 3. This addition is followed by a migration of the bulky $Si(SiMe_3)_3$ group onto the isocyanide carbon. Alternatively, the first ArNC may add trans to the silyl ligand (among the three neopentyl ligands). However, such addition is expected to, in contrast to the experimental observations, be followed by a neopentyl migration and the formation of a Zr−C insertion product. Only up to three isocyanide insertions occur in **1** and **2** to give **7** and **8**. This is perhaps due to steric crowding around the metal atom in **7** and **8** hindering further ArNC coordination.

In summary, the isocyanide insertion into Zr−silyl bonds is preferred in the reactions of Cp-free $(Me_3ECH_2)_3ZrSi(SiMe_3)_3$ [E = C (**1**), Si (**2**)] with ArNC, and it is the first step in the multi-insertion reactions. Steric congestion may limit the number of isocyanide insertions, as observed in the inertness of the tri-insertion products **7** and **8** toward further ArNC insertion.

Acknowledgment is made to the National Science Foundation (Grant CHE-9457368), the DuPont Young Professor Award, the Camille Dreyfus Teacher-Scholar Award, the donors of the Petroleum Research Fund, administered by the American Chemical Society, and Exxon Education Foundation for support of this research. We thank Professor Arnold L. Rheingold and a referee for helpful suggestions.

Supporting Information Available: A complete list of crystallographic data for **1**, **3**, and **7** (24 pages). See any current masthead page for ordering information.

OM980485O